



Highly selective and stable Cu/SiO₂ catalysts prepared with a green method for hydrogenation of diethyl oxalate into ethylene glycol



Jie Ding^{a,b}, Tiberiu Popa^{a,d,e}, Jinke Tang^c, Khaled A.M. Gasem^a, Maohong Fan^{a,d,e,*}, Qin Zhong^{b,**}

^a Department of Chemical and Petroleum Engineering, University of Wyoming, Laramie, WY 82071, USA

^b School of Chemical Engineering, Nanjing University of Science and Technology, Nanjing, Jiangsu 210094, PR China

^c Department of Physics and Astronomy, University of Wyoming, Laramie, WY 82071, USA

^d School of Energy Resources, University of Wyoming, Laramie, WY 82071, USA

^e School of Civil and Environmental Engineering, Georgia Institute of Technology, Mason Building, 790 Atlantic Drive, Atlanta, GA 30332, USA

ARTICLE INFO

Article history:

Received 14 October 2016

Received in revised form 20 February 2017

Accepted 22 February 2017

Available online 6 March 2017

Keywords:

Cu/SiO₂

Ammonium carbonate

Green method

Diethyl oxalate hydrogenation

Ethylene glycol

ABSTRACT

Dimethyl oxalate (DMO) hydrogenation for ethylene glycol (EG) production is problematic due to environmental concerns and safety regulations. Therefore, development of improved methods for diethyl oxalate (DEO) hydrogenation based EG production is desirable. The objective of this research was to develop a cost-effective and environmentally benign approach for the synthesis of highly active and stable Cu/SiO₂ catalysts for selective hydrogenation of diethyl oxalate (DEO) to ethylene glycol (EG). Here, ammonium carbonate is used to prepare Cu/SiO₂ catalysts through deposition precipitation instead of the conventional pollution-producing evaporation process associated with the use of ammonia. The Cu/SiO₂ catalysts prepared with the new method achieved 6.9–13.1% higher selectivity and showed better stability. The improved stability and selectivity resulted from increased chemical adsorption of DEO and H₂ due to the high Cu₂O concentration and Cu⁺/(Cu⁰ + Cu⁺) ratio (reduced from ion-exchanged Cu—O—Si units), and reduced carbon deposition on the Cu/SiO₂ catalyst. The Cu₂O reduced from Cu—O—Si units in the Cu/SiO₂ catalyst prepared by the new method was more stable than the Cu⁺ species reduced from copper phyllosilicate in the Cu/SiO₂ catalyst prepared by the conventional method. Therefore, the new Cu/SiO₂ catalyst preparation method appears most promising.

© 2017 Elsevier B.V. All rights reserved.

1. Introduction

Ethylene glycol (EG) has become an increasingly important chemical for many industries. Therefore, development of new cost-effective methods for its production has attracted significant attention. Researchers are currently interested in dimethyl oxalate (DMO) hydrogenation [1–6]. Versatile copper-containing catalysts were used extensively in vapor-phase hydrogenation of DMO to EG [1,2,7–10], some of which (such as copper-chromium catalysts) became the preferred industrial catalysts for the DMO-to-EG process because of the relatively high catalytic stability and long lifespans [11]. However, the toxic chromium catalysts are dangerous and inconvenient for practical applications, consider-

ing the environmental requirements and the safety of the workers. Recently, silica-supported copper catalysts (Cu/SiO₂) have demonstrated not only outstanding ability for hydrogenation of DMO to EG, but also low cost and safety characteristics [1,12–16].

Most of the Cu/SiO₂ catalysts are prepared by the ammonia-evaporation method, which includes mixing of copper nitrate with ammonia at pH ~11 to form teraamino cupric complex, adding of silica sol, and boiling of the suspension until the pH reaches 6–7 for the copper compound precipitation. The catalysts prepared by ammonia evaporation method possess a high initial surface areas and high content of copper phyllosilicate [1,17]. It has been reported that the catalytic activity and stability in DMO hydrogenation to EG are mainly attributed to three reasons. The surface compositions, including the contents of copper species and silica, represent the first reason. Wen et al. and Yin et al. have reported that the silica loss of Cu/SiO₂ during the reaction or the copper loading reduction can result in the apparent decline of the catalytic activity and stability [18,19]. The second is the dispersion of copper species. The copper phyllosilicate and large surface areas have been

* Corresponding author at: Department of Chemical and Petroleum Engineering, University of Wyoming, Laramie, WY 82071, USA.

** Corresponding author.

E-mail addresses: mfan@uwyo.edu (M. Fan), zq304@mail.njust.edu.cn (Q. Zhong).

reported to benefit the dispersion of copper species [11,20–23]. Lin et al. have inhibited the agglomeration of copper species by using ethanol for stabilization or by introducing dispersion-beneficial supports to enhance the catalytic activity [20,24–27]. The third reason is the surface having high Cu⁺ and Cu⁰ concentrations and Cu⁺/(Cu⁰ + Cu⁺) ratio. Wang et al. and Gong et al. have found that the cooperative effect between Cu⁰ and Cu⁺ is responsible for the good hydrogenation over Cu/SiO₂, where Cu⁰ mainly facilitates the H₂ decomposition while the Cu⁺ sites chemically adsorb the organics [21,28,29]. Therefore, the silica-supported copper catalysts with high copper phyllosilicate concentrations, good dispersions of surface copper species, large surface areas, and high Cu⁰ and Cu⁺ concentrations combined with high Cu⁺/(Cu⁰ + Cu⁺) ratio could achieve a good performance in DMO hydrogenation to produce EG. The Cu/SiO₂ catalysts prepared by ammonia evaporation method can also produce a good DMO hydrogenation to EG [1,17] due to the high initial surface areas and copper phyllosilicate concentration. However, the process remains environmentally unfriendly because of ammonia evaporation during the catalyst preparations. Therefore, this research team developed and reported a new method for Cu/SiO₂ preparation utilized in DMO hydrogenation to EG in 2015 [30]. Ammonium carbonate was used as the precipitation agent for the preparation of Cu/SiO₂ catalysts via deposition-precipitation method. This procedure not only apparently decreased the environmental pollution by reducing ammonia evaporation, but also obtained higher catalytic activity and stability for DMO hydrogenation to EG. Although such hydrogenation has been well developed, the application of this technology in the U.S. remains limited because of environmental concerns and safety regulations. Therefore, initiating the effort in developing new EG production technology is important. Diethyl oxalate (DEO) is a safe, non-explosive and environment-friendly oxalate that can provide a good alternative in hydrogenation to EG [3,31]. Further, finding a good catalyst which is prepared by a green method with high and stable activity for DEO hydrogenation is of great significance. However, to date, rare efforts have been made in the study of vapor-phase DEO hydrogenation [3,31], which is far from being completely investigated.

Herein, the research team developed a cost-effective and environmentally benign method to synthesize the Cu/SiO₂ by further improving the method reported in 2015 [30] for DEO hydrogenation to EG. Compared to the previous study [30], this investigation mainly focused on delineating the reasons for higher Cu/SiO₂ catalytic performance and stability when prepared by the new method. In addition, in clear contrast to DMO hydrogenation by the ammonia evaporation method (AEM), the catalysts prepared by deposition-precipitation approach possessed lower copper phyllosilicate concentrations, smaller BET surface areas, poorer dispersion of copper species and lower surface copper composition. Nevertheless, these characteristics achieved higher DEO hydrogenation and better stability. In this study, the catalytic processes involving Cu/SiO₂ prepared by the new and conventional methods were systematically investigated to analyze the above phenomenon.

2. Experimental

2.1. Catalyst preparations

The Cu/SiO₂ catalysts were prepared by two methods. One was the ammonium carbonate-based deposition-precipitation method ((NH₄)₂CO₃ DPM) reported by our group previously with some modifications [30]. Briefly, in this method Cu(NO₃)₂·2.5H₂O, HNO₃ and H₂O were mixed to form 8.0 wt% (copper) solutions at pH ~1. The silica sol [LUDOX® AS-30 colloidal silica 30% ammonia

stabilized/Cu(NO₃)₂·2.5H₂O = 3.28 (mass ratio) or LUDOX® AM-30 colloidal silica 30%, sodium stabilized/Cu(NO₃)₂·2.5H₂O = 3.31, silica in water, Sigma-Aldrich] and (NH₄)₂CO₃-saturated solution were added under stirring. The obtained suspension was filtered, washed, dried and calcined in air at 450 °C for 4 h. The resulting catalysts were designated as Cu-AS-AC and Cu-AM-AC, respectively.

The other procedure was the AEM. Here, Cu(NO₃)₂·2.5H₂O, ammonia and H₂O were mixed to form 8.0 wt% (copper) solutions at pH ~10–11. The silica sol (Silica sol LUDOX® AS-30 colloidal silica 30% silica in water/Cu(NO₃)₂·2.5H₂O = 3.31, ammonia stabilized, Sigma-Aldrich) was added under stirring, and the temperature was raised to 90 °C for the evaporation of ammonia until pH ~6–7. The precipitates were filtered, washed, dried and calcined in air at 450 °C for 4 h. The resulting catalyst was denominated as Cu-AS-AE.

2.2. Characterization of catalysts

The total metal loading of the catalysts was analyzed by inductively coupled plasma spectrometry (ICP) using PerkinElmer Optima 8300 ICP-OES Spectrometer. N₂ adsorption isotherms were performed on a volumetric system Autosorb IQ ASIQCO100-4 Quantachrome Instruments. X-ray diffraction (XRD) tests were performed at the scanning speed of 8°/min from 10° to 90° with 0.02° step on a Rigaku Smartlab XRD system. The thermogravimetric analyses (TGA) were carried out on a SDT Q600 thermogravimetric analyzer at the temperature rate of 10 °C/min from 50 °C to 1000 °C under nitrogen (100 mL/min) or 20 vol.% oxygen/nitrogen (120 mL/min). The infrared (IR) spectra were recorded on a Nicolet 6700 spectrometer with a spectral resolution of 4 cm⁻¹. X-ray photoelectron spectroscopy (XPS) and X-ray-excited Auger electron spectroscopy (XAES) were conducted using a Kratos Axis Ultra DLD X-ray photoelectron spectrometer with a monochromated Al K-alpha source running at 150 W. To avoid the reoxidation during the XPS tests, the samples were sealed in the sample bottle with full N₂ and fixed in the XPS vacuum chamber in ten minutes after reduction. Hydrogen temperature-programmed reduction (H₂-TPR) or temperature-programmed desorption (H₂-TPD) tests were performed on a Autosorb IQ ASIQCO100-4, quantachrome instrument, equipped with thermal conductivity detector (TCD). H₂-TPR was carried out in the mixture of 5 vol.% H₂–95 vol.% He (US Welding) with temperature increasing at 10 °C/min to 900 °C. H₂-TPD was performed on catalysts after an initial 350 °C reduction in 95 vol.% H₂–5 vol.% Ar for 6 h and then the adsorption was conducted at 40 °C with 100 vol.% H₂, and finally the desorption was programmed at 10 °C/min to 900 °C in flowing Ar. The morphology of the catalysts was studied by transmission electron microscopy (TEM) using FEI-Tecnai G2 F20 S-Twin 200 kV equipment. The particle size distribution was calculated on monolayer particles by using Image J 1.48v and Icy 1.5.3.0 software. The in situ IR spectra were recorded on a Nicolet 6700 spectrometer with a resolution of 4 cm⁻¹. All samples were reduced under an 95 vol.% H₂–5 vol.% N₂ flow at 350 °C for 6 h in the cell. The cell was then evacuated for 30 min to remove the physisorbed hydrogen species. Afterwards, the temperature of the sample was reduced to reaction temperature, and the DEO vapor together with N₂ (UHP, US Welding) was introduced into in situ cell, with the temperature ranging from 220 to 320 °C.

2.3. Catalytic activity tests

The catalytic performance of vapor-phase DEO hydrogenation was evaluated using a fixed-bed experimental set-up, as shown in Fig. 1. Typically, 930 mg of Cu-AS-AC or Cu-AM-AC or Cu-AC-AE was loaded into the center of the reaction tube (11 mm inner diameter and 500 mm length). All three catalysts have similar densities. The catalyst was reduced under 95 vol.% H₂–5 vol.% N₂ flow

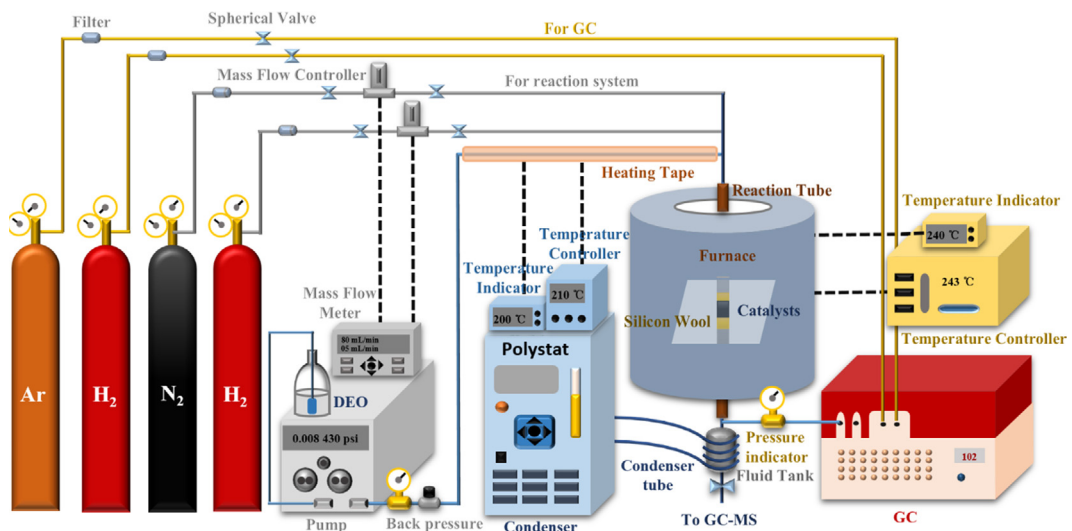
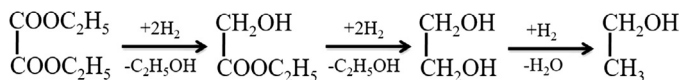


Fig. 1. Schematic of the experimental set-up used for catalytic activity and stability testing.



Scheme 1. Reaction pathway for the hydrogenation of DEO to EGly, EG and ethanol.

(120 mL/min) at 350 °C for 6 h at the pressure of 2.9 MPa. The temperature and pressure were then decreased to the desired reaction temperature (200–280 °C) and reaction pressure (2.0–2.9 MPa). The liquid DEO (0.008 mL/min, Certified ACS >99.8%, Sigma-Aldrich) was pumped into the reactor. Gaseous products were analyzed by online gas chromatograph SRI 8610C equipped with two Restek-packed columns and a capillary column, while liquid products were collected and analyzed by offline GC-MS Agilent 7890A GC system-5975CVL MSD using an Agilent HP-5MS (30 m × 0.250 mm) capillary column equipped with automatic liquid sampler (ALS). Every catalyst was repeatedly tested for three times and the error bar was calculated.

3. Results and discussions

3.1. Catalytic activity and stability

The catalytic activity and stability of Cu-AS-AC, Cu-AM-AC and Cu-AS-AE were investigated in DEO hydrogenation, which proceeded via ethyl glycolate (EGly) to EG, while EG could be dehydrated further to ethanol (**Scheme 1**). Other products like 2-butanol may also be generated [31,32]. To compare the catalytic properties of all three catalysts, the effect of reaction temperature, reaction pressure, liquid hourly space velocity (LHSV) and long-term catalytic stability was investigated. It should be noted that the Carberry and Wheeler-Weisz numbers for DEO hydrogenation process indicate that the mass transfer limitations could be negligible [12,17]. Details are given in Section S1 of the Supporting Information.

3.1.1. Effect of reaction temperature

The variations of catalytic activities over Cu-AS-AC, Cu-AM-AC and Cu-AS-AE at the reaction temperatures of 200–280 °C, reaction pressure of 2.9 MPa, and LHSV of 1.0 mL_{DEO} mL_{cat}⁻¹ h⁻¹ are shown in **Fig. 2a**. The DEO conversions increase slightly with the reaction temperature and reach >99% at 240 °C. However, the EG selectivity initially increases up to the maximum value at 240 °C, and it then decreases with increasing reaction temperature. The increase of the EG selectivity may be caused by the promotion of the reac-

tion between H₂ and DEO due to rising reaction temperature, but further increase in temperature results in more side reactions such as dehydration [12], as indicated by Fig. S1. As shown in Fig. S1, it can be inferred that the peak area of the side products like ethyl ether, 2-butanol, etc. at 260 °C are apparently larger than those at 240 °C. The EG selectivity of Cu-AS-AC ranges from 73.2% to 95.5%, while that of Cu-AS-AE and Cu-AM-AC achieve only 63.4–85.0% and 45.2–84.4%, respectively. Wang et al. have reported that in their study, the DEO conversion increased up to 76% with the reaction temperature, while the EG selectivity first increased up to 40% at 240 °C and then decreased; thus, they agree with the results of this study but show lower conversion and selectivity [31]. Ding et al. have also reported the DEO conversion and EG selectivity at 220 °C and 270 °C [3], and the results showed that conversion and selectivity at 220 °C were much higher than that at 270 °C.

3.1.2. Effect of reaction pressure

The effect of reaction pressure on the DEO conversion and EG selectivity was tested at the reaction temperature of 240 °C, reaction pressures of 2.0–2.9 MPa, and LHSV of 1.0 mL_{DEO} mL_{cat}⁻¹ h⁻¹, as shown in **Fig. 2b**. The DEO conversions increased up to 99% at pressures >24 MPa. The EG selectivity was enhanced with the reaction pressure. Specifically, Cu-AS-AC exhibited the highest EG selectivity (71–95%), whereas Cu-AS-AE displayed the lowest values (59–84%) and Cu-AM-AC showed 69–85% EG selectivity. Wang et al. have also reported the increase of both DEO conversion and EG selectivity with the reaction pressure [31]. However, in contrast to this study, the DEO conversion and EG selectivity in Wang et al.'s study initially increased up to the maximum value at 1.0 MPa and then remained constant. This behavior could have been caused by different catalyst preparations and different reaction conditions. Further, the molar ratio of H₂/DEO was as high as 200 in Wang's report, which was 2.5 times higher than that in this study.

3.1.3. Effect of LHSV

The catalytic properties of Cu-AS-AC, Cu-AM-AC and Cu-AS-AE examined at the reaction temperature of 240 °C, reaction pressure of 2.9 MPa and LHSV of 1.0–2.0 mL_{DEO} mL_{cat}⁻¹ h⁻¹ are presented in **Fig. 2c**. Both DEO conversion and EG selectivity decreased with the LHSV. Cu-AS-AC exhibited the highest DEO conversion and EG selectivity, which was 99% and 95% at the LHSV of 1.0 mL_{DEO} mL_{cat}⁻¹ h⁻¹, respectively. The DEO conversion and EG selectivity on Cu-AM-AC were lower, 98% and 85% at the LHSV of 1.0 mL_{DEO} mL_{cat}⁻¹ h⁻¹, respectively. Although the conversion and

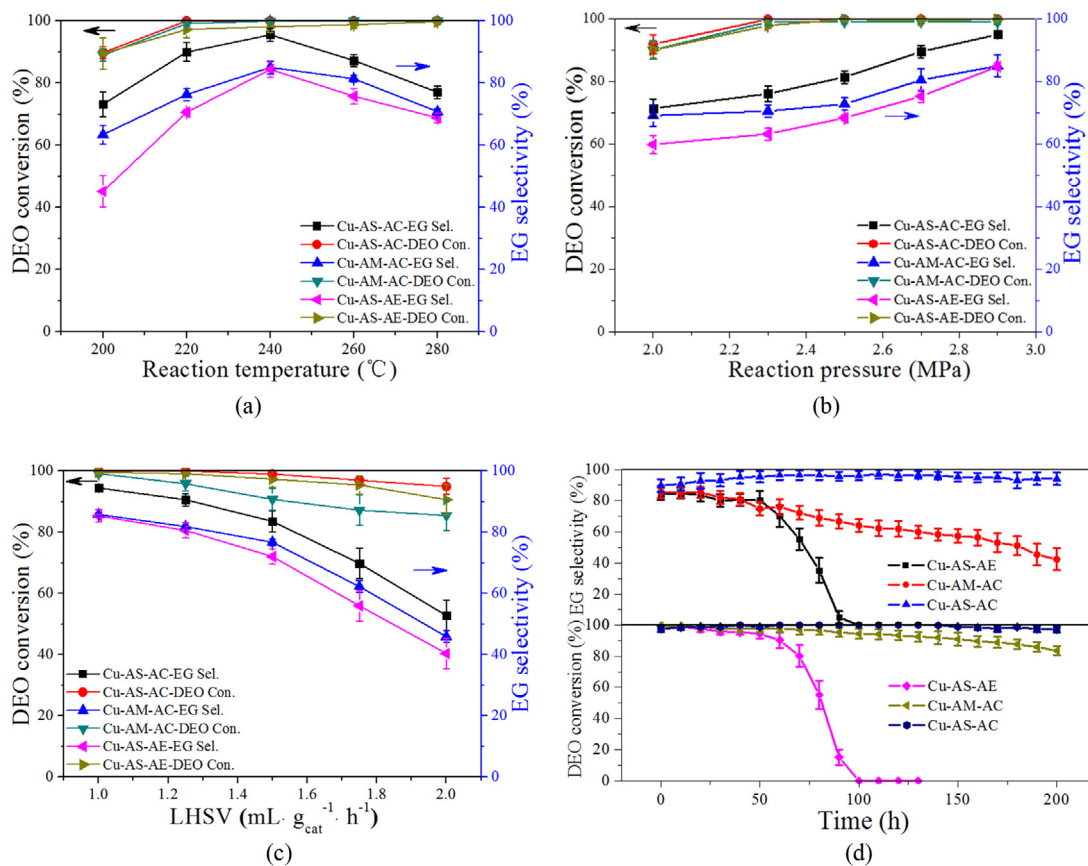


Fig. 2. Effect of (a) reaction temperature, (b) reaction pressure and (c) LHSV on DEO conversion and EG selectivity as well as (d) the long-term stability of EG selectivity and DEO conversion.

selectivity on Cu-AS-AE were close to the ones for Cu-AM-AC at the LHSV of $1.0 \text{ mL g}_{\text{cat}}^{-1} \text{ h}^{-1}$, they were decreased further apparently with increasing LHSV. The decrease of DEO conversion and EG selectivity with LHSV has also been reported by Ding et al. and Wang et al. [3,31].

3.1.4. Catalytic stability

The long-term stability of Cu/SiO₂ catalysts is important for vapor-phase DEO hydrogenation to EG from both academic and industrial viewpoints. A comparison of long-term catalytic stability of Cu-AS-AC, Cu-AM-AC and Cu-AS-AE is tested and presented in Fig. 2d. Cu-AS-AC showed excellent performance and stability in both DEO conversion and EG selectivity, which remained over 97% and 92% for 200 h, respectively. In contrast, obvious deactivation of Cu-AS-AE was observed within 100 h under identical reaction conditions. Such deactivations have been reported in many other literatures [33–35]. Cu-AM-AC exhibited gradual decrease of DEO conversion and EG selectivity from 99% and 85% to 80% and 40%, respectively.

From the above results, it can be obtained that Cu-AS-AC not only has the highest DEO conversion but the best EG selectivity among the three catalysts, but also it helps achieve excellent long-term catalytic activity and stability. Further, while Cu-AM-AC shows a little worse catalytic activity and stability, it is still much better than the catalyst prepared by AEM. The results obtained also indicate that the catalytic performance is dramatically improved in the Cu/SiO₂ prepared by (NH₃)₂CO₃ DPM. These three catalysts were investigated to analyze the reasons behind their observed diverse performance and catalytic stability.

Table 1
Catalyst yields of Cu-AS-AC, Cu-AM-AC and Cu-AS-AE.

Sample	Cu-AS-AC	Cu-AM-AC	Cu-AS-AE
Yields (%)	91.5	91.1	60.8

3.2. Physiochemical properties of catalysts

A number of previous studies have reported that the physicochemical properties of the catalysts, including surface compositions, surface areas and dispersions of copper species, play an important role in the DMO hydrogenation [1,3,12,19,31]. Therefore, they were investigated in this study.

3.2.1. Catalyst yields

The catalyst yields were calculated from Eq. (1) and listed in Table 1.

$$Y = \frac{m_p}{m_0} \quad (1)$$

Here m_p represents the mass of catalysts and m_0 represents the theoretical mass of catalysts. As shown in Table 1, the yields of Cu-AS-AC and Cu-AM-AC achieved over 91.0%, while that of Cu-AS-AE obtained only 60.8%. The ammonium ions can react with copper ions in the solutions to form highly soluble Cu(NH₃)₄⁺, leading to the loss of copper species when filtration and washing in the catalyst preparations. Previous researchers have also reported the loss of copper species in the AEM [18,36], which mainly led to the low copper loading. However, in this study, it was interesting that the copper loading in Cu-AS-AE (Table 2) was close to the one in Cu-AS-AC and Cu-AM-AC, which reaches over 18.0% but is lower than the preset one (20%). This indicates that the loss of copper

Table 2

Copper loading of Cu-AS-AC, Cu-AM-AC and Cu-AS-AE.

Sample	Cu (wt%)	Si (wt%)	Cu/Si (wt/wt)
Cu-AS-AC	18.2	36.1	0.5042
Used Cu-AS-AC	18.0	36.1	0.4986
Cu-AM-AC	18.7	35.7	0.5238
Used Cu-AM-AC	19.1	35.6	0.5365
Cu-AS-AE	18.2	36.2	0.5028
Used Cu-AS-AE	18.5	36.1	0.5125

Table 3

Weight of catalysts before and after reaction.

Samples	Before reaction	After reaction
Cu-AS-AC	0.500 g	0.495 g
Cu-AM-AC	0.500 g	0.492 g
Cu-AS-AE	0.500 g	0.413 g

Table 4

Mass coverage (wt%) on the catalyst surfaces resulting from XPS (Cu2p) peak deconvolution.

Samples	Cu ²⁺	Cu ⁺	Cu ⁰	T(Cu)	T(Cu ⁰ +Cu ⁺)	Cu ⁺ /(Cu ⁰ +Cu ⁺)
Cu-AS-AC						
Fresh	11.6	0		11.6	0	–
Reduced	0	9.0	4.1	13.1	13.1	0.69
Used	0	9.0	3.9	12.9	12.9	0.70
Cu-AM-AC						
Fresh	10.8	0		10.8	0	–
Reduced	0	8.3	4.7	13.0	13.0	0.64
Used	5.5	3.4	1.6	10.5	5.0	0.32
Cu-AS-AE						
Fresh	27.8	0		27.8	0	–
Reduced	0	8.0	6.0	14.0	14.0	0.57
Used	6.8	1.0	0.6	8.5	1.6	0.12

Note: T(Cu) is the total surface content of Cu, obtained from XPS characterization; and T(Cu⁰+Cu⁺) is the total surface content of (Cu⁰+Cu⁺).

species occurs in the Cu/SiO₂ even prepared by (NH₃)₂CO₃ based deposition-precipitant method, whereas both copper species and silica are lost in the AEM, which may be caused by the higher concentration of ammonia ions in the AEM. This further confirms the environmentally benign properties of (NH₃)₂CO₃ DPM.

3.2.2. Chemical compositions

Copper loading of the fresh and used catalysts were determined using ICP-OES as shown in Table 2. The theoretical copper loading (TCL) was calculated according to Eq. (2) to be ~20%.

$$\text{TCL} = \frac{m_{\text{Cu}}}{m_{\text{CuO}} + m_{\text{SiO}_2}} \quad (2)$$

It is clear that the copper loading found by ICP-OES is a little lower than the theoretical values for all the three catalysts. The copper loading and silica content of the fresh catalysts were hardly changed compared with the used ones, indicating that copper or silica, or both, is seldom lost in the vapor-phase DEO hydrogenation. To further ascertain whether they are lost or not, the weight of catalysts before and after reaction are shown in Table 3. It can be seen that Cu-AS-AE exhibited apparent weight loss after reaction, suggesting the loss of both copper species and silica. However, Cu-AS-AC and Cu-AM-AC hardly exhibited any weight loss, illustrating the stability of catalysts in the reactions and the environmental benign properties of (NH₃)₂CO₃ DPM.

3.2.3. Surface compositions

The surface compositions of copper species and silica were calculated from XPS and XAES spectra, as shown in Table 4. The content of surface copper species of Cu-AS-AC and Cu-AM-AC were 11.6%

and 10.8%, respectively, lower than those tested by ICP-AES. However, the content of copper species on the surface of Cu-AS-AE was 27.8% higher than the one tested by ICP-AES. The Cu/SiO₂ prepared by AEM generally produced copper phyllosilicates with 20–40 nm length rods [21,39]. After being reduced, the content of copper species in Cu-AS-AC and Cu-AM-AC slightly increased to 13.1% and 13.0%, respectively, whereas the content in Cu-AS-AE dramatically decreased to 13.9%. The content of copper species in all three catalysts decreased after being used. This decrease is most probably attributed to the carbon deposition during the hydrogenation [37] because the XPS can only test the 10 nm thickness surface copper species.

3.2.4. BET surface area

The specific surface areas of fresh and used catalysts are listed in Table 5. The fresh Cu-AS-AE produced the largest BET surface area and highest pore volume, 363.9 m²/g and 1.29 cm³/g, respectively, which decreased to 283.5 m²/g and 1.06 cm³/g after being used. Cu-AS-AC had the smallest BET surface area and pore volume, 158.8 m²/g and 0.52 cm³/g, respectively, which decreased to 152.2 m²/g and 0.48 cm³/g after being used. Cu-AM-AC presented 187.4 m²/g BET surface area and 0.88 cm³/g pore volume, and they decreased to 155.2 m²/g and 0.88 cm³/g after being used. It can be concluded that the surface areas and pore volumes are in the following decreasing order: Cu-AS-AE > Cu-AM-AC > Cu-AS-AC, which has the opposite trend to catalytic activities. This suggests that BET surface areas and pore volumes play a weak role in the vapor-phase DEO hydrogenation, although a number of researchers have successfully improved the catalytic performance and stability in DMO hydrogenation by increasing the surface areas [3,12,20]. It indicates that there are some differences between the DEO hydrogenation and DMO hydrogenation.

3.2.5. TEM images

The TEM images of fresh, reduced and used catalysts are shown in Fig. 3. In the TEM images of fresh catalysts, dark spherical particles are dispersed on light-gray particles for Cu-AS-AC and Cu-AM-AC. The former is recognized as the copper species and the latter is silica, as indicated in previous studies [19,21,38]. However, a number of elongated copper phyllosilicate particles were observed in Cu-AS-AE images, which is in agreement with earlier analyses [21,39,40]. These observations further support the high content of copper species on the surface of fresh Cu-AS-AE. After being reduced, all three catalysts showed the spherical particles of copper species dispersed well on the silica. It is possible that a part or all of copper phyllosilicates in Cu-AS-AE were decomposed by H₂; in such case, the decomposed Cu-AS-AE generates the spherical particles, which disperse on the silica and migrate into the pores of silica. Further, the copper species on reduced Cu-AS-AC agglomerated to form the largest particles among the three catalysts, while the reduced Cu-AS-AE exhibits the smallest ones, indicating that copper phyllosilicate is beneficial for the well dispersion of copper species, consistent with previous studies [21,41]. After being used, Cu-AS-AC and Cu-AM-AC show hardly any change in copper species, while Cu-AS-AE exhibits a slight aggregation. The distribution of copper species is calculated as shown in Fig. 3d–f. It is obvious that the dispersion of copper species on reduced catalysts decreased as follows: Cu-AS-AE > Cu-AM-AC > Cu-AS-AC. It should be noted that although the copper species in reduced Cu-AS-AE show a better dispersion than those in reduced Cu-AS-AC and Cu-AM-AC, they are aggregated in similar sizes with the latter two after being used. This could perhaps explain the poor catalytic stability of Cu-AS-AE.

Above all, the new method for DEO hydrogenation to EG exhibited a more environmentally benign nature than the conventional one. The variation of physicochemical properties of fresh, reduced

Table 5
Specific surface areas for catalysts.

Samples	BET surface area (m^2/g)	BJH total pore volume (cm^3/g)	BJH average pore diameter (nm)
Cu-AS-AC	158.8	0.52	9.5
Used Cu-AS-AC	152.2	0.48	12.3
Cu-AM-AC	187.4	0.88	12.3
Used Cu-AM-AC	155.2	0.73	12.2
Cu-AS-AE	363.9	1.29	3.1
Used Cu-AS-AE	283.5	1.06	3.2

and used catalysts were not consistent with the differences in catalytic activities. Specifically, the content of surface copper species in the reduced Cu-AS-AE was higher than those of Cu-AS-AC and Cu-AM-AC. The BET surface area and pore volume of Cu-AS-AE were larger than those of Cu-AM-AC and Cu-AS-AC. The copper species in reduced Cu-AS-AE were dispersed better than the ones in reduced Cu-AS-AC and Cu-AM-AC. However, the catalytic activities of Cu-AS-AC and Cu-AM-AC were higher than those of Cu-AS-AE, which indicates that the physicochemical properties of catalysts play a weak role in the DEO hydrogenation to EG.

3.3. Copper species on catalysts

In contrast to previous approaches for DMO hydrogenation to EG [12,20,21], the physicochemical properties of the Cu/SiO₂ in the present study played a weak role in the DEO hydrogenation to EG. In addition, it has been reported that copper species like copper phyllosilicate in the catalysts may promote the DMO hydrogenation [21,42,43]. Therefore, the copper species on DEO hydrogenation were investigated in this study.

3.3.1. XRD analysis

Fig. 4a presents the XRD patterns of the fresh and reduced Cu-AS-AC, Cu-AM-AC and Cu-AS-AE. Sharp diffraction peaks at $2\theta = 33.4^\circ, 35.6^\circ, 38.8^\circ, 48.8^\circ, 61.5^\circ, 66.2^\circ$ and 68.1° in the fresh Cu-AS-AC are assigned to CuO, and the fresh Cu-AM-AC shows the same but weaker and wider peaks, indicating that the CuO particles in Cu-AS-AC are larger than those in Cu-AM-AC. These results are consistent with the TEM findings. In comparison, the fresh Cu-AS-AE hardly displays any CuO peaks. From the analysis of TEM images, it can be concluded that Cu-AS-AE is probably composed of mainly copper phyllosilicate, which shows poor crystallinity as other researchers have reported [21,41]. A fraction of copper phyllosilicate may undergo decomposition during calcination, resulting in well dispersed CuO accompanied by intact copper phyllosilicate [21,44], and both are invisible in fresh Cu-AS-AE. The peak at $2\theta = 22.0^\circ$ belongs to the amorphous silica. After reduction, Cu-AS-AC and Cu-AM-AC show a strong diffraction peak at $2\theta = 43.3^\circ$ along with three weak ones at $50.4^\circ, 74.1^\circ$ and 85.0° characteristic of Cu⁰, and a weak and broad peak at around 36.4° ascribable to the Cu₂O (111) plane can also be observed, indicating that at least Cu₂O and Cu⁰ are present in Cu-AS-AC and Cu-AM-AC. The reduced Cu-AS-AE only shows two peaks at 36.4° and 42.5° corresponding to Cu₂O (111) and Cu₂O (200), and the peaks are weaker than Cu-AS-AC and Cu-AM-AC, suggesting that a part of copper phyllosilicate may be reduced into Cu₂O, and there may be other Cu⁺ species. It was reported that the reduction of copper phyllosilicate ceased at Cu⁺ under the present reduction conditions due to the strong interaction between copper ions and SiO₂ [21,28].

3.3.2. IR analysis

Fig. 4b shows the IR spectroscopy of fresh and reduced Cu-AS-AC, Cu-AM-AC and Cu-AS-AE. It has been reported that the formation of copper phyllosilicate is supported by the appearance of the δ_{OH} band at 663 cm^{-1} and the ν_{SiO} shoulder peak at 1040 cm^{-1} . The peaks at 800 cm^{-1} and 1110 cm^{-1} correspond to

the ν_{SiO} asymmetric and ν_{SiO} symmetric stretching bands of SiO₂, respectively [21,28]. The stretching vibrations of copper oxides are generally observed at ca. 490 cm^{-1} [45,46]. All the three catalysts including fresh and reduced catalysts show the apparent peaks at $1110\text{ cm}^{-1}, 800\text{ cm}^{-1}$ and 490 cm^{-1} , illustrating the existence of SiO₂ and copper oxides in the catalysts. It can be noted that the fresh Cu-AS-AE exhibits the peak at 1040 cm^{-1} and 663 cm^{-1} , suggesting the presence of copper phyllosilicate. Evidently, a peak at 969 cm^{-1} is observed in the fresh Cu-AS-AC and Cu-AM-AC, which is attributed to the ion-exchanged Cu—O—Si units as previously reported [47,48]. The ion-exchanged method reported by Kobayashi et al. [49] and Kohler et al. [50] resembles to some extent the (NH₄)₂CO₃ DPM used here, because the SiO₂ is immersed in the Cu(NH₃)₄²⁺ solution in all the above methods. Although most of Cu²⁺ was combined with CO₃²⁻ in the (NH₄)₂CO₃ DPM, there still existed some dissociated Cu²⁺ in the solution because the color of the solution was dark blue even after adding of (NH₄)₂CO₃. The copper species in the Cu/SiO₂ catalysts prepared by the ion-exchange method were presented in two forms. One was the immobilized single copper ions on SiO₂ surface by exchanging with two silanol groups, and the other was a well dispersed CuO over the ion-exchanged Cu—O—Si units [21]. Thus, in Cu-AS-AC and Cu-AM-AC, besides the presence of CuO particles identified by XRD and TEM, there were ion-exchanged Cu—O—Si units and well dispersed CuO. The formation of large CuO particles is attributed to the aggregation of some loosely binding well dispersed CuO and the decomposition of CuCO₃ during calcination. Compared to the fresh Cu-AS-AC, the reduced one hardly showed peaks of ion-exchanged Cu—O—Si units, suggesting the complete reduction. It has been reported that the ion-exchanged Cu—O—Si units and copper phyllosilicate were only reduced into Cu⁺ at a temperature lower than 600°C [21]. However, the reduced Cu-AM-AC and Cu-AS-AE not only showed the peaks of copper oxides and SiO₂ but also exhibited the peak at 969 cm^{-1} . Especially, the reduced Cu-AS-AE obtained the highest peak at 969 cm^{-1} , which may be from a similar Cu—O—Si units from the reduction of copper phyllosilicate.

3.3.3. TGA analysis

Fig. 4c shows the effect of temperature on $\Delta h/\Delta T$ for the fresh and reduced Cu-AS-AC, Cu-AM-AC and Cu-AS-AE. The fresh Cu-AS-AC and Cu-AS-AE show apparent peaks at 940°C and 890°C , respectively. The former peak is attributed to the transformation of CuO into Cu₂O [51]. The weight loss over ca. $800\text{--}950^\circ\text{C}$ in the TGA spectra as shown in Fig. 4d further confirms the transformation of CuO into Cu₂O. The latter one is assigned to the decomposition of copper phyllosilicate [52]. The weight loss (Fig. 4d) in the temperature range of $765\text{--}890^\circ\text{C}$ supports the decomposition of copper phyllosilicate. The fresh Cu-AM-AC exhibits both peaks at 890°C and 940°C , indicating the existence of copper phyllosilicate and CuO. The fresh Cu-AM-AC exhibits similar TGA curves to the fresh Cu-AS-AC, but shows larger weight loss. This is because Cu-AM-AC contains not only similar amount of CuO compared to Cu-AS-AC but also copper phyllosilicate. It is interesting that the ion-exchanged Cu—O—Si units are not observed in the TGA curves, which may be due to the stable structures formed from the strong interaction between copper oxides and SiO₂. After reduction, it can be seen

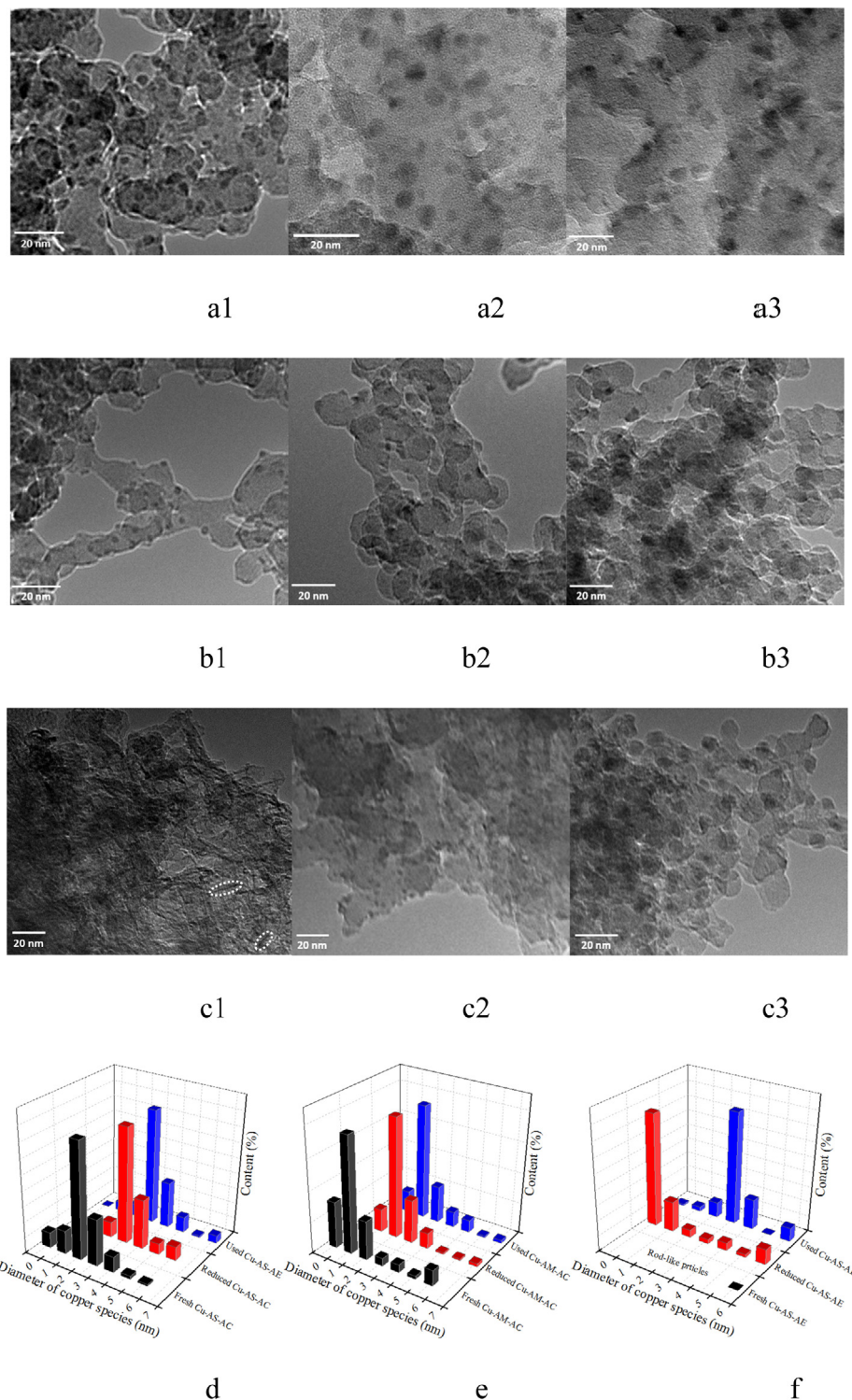


Fig. 3. TEM images of Cu-AS-AC, Cu-AM-AC and Cu-AS-AE. (a) Cu-AS-AC, (b) Cu-AM-AC and (c) Cu-AS-AE; (1) fresh, (2) reduced, (3) used; (d) dispersion of copper species in Cu-AS-AC, (e) dispersion of copper species of Cu-AM-AC, (f) dispersion of copper species of Cu-AS-AE.

that the peaks corresponding to CuO and copper phyllosilicate disappeared, while a new peak with weaker intensity at 880 °C was observed for the reduced copper phyllosilicate, where Cu²⁺—O—Si units were reduced to Cu⁺—O—Si units as indicated by previous papers [21,36]. In the copper phyllosilicate, there are a number of surface —OH linked to Cu²⁺—O—Si units and the surface —OH can

easily combined with H₂ to be reduced. More details on this are given in the following section.

3.3.4. XPS analysis

To further analyze the copper species in fresh and reduced Cu-AS-AC, Cu-AM-AC and Cu-AS-AE, the Cu2p XPS spectra were conducted, as shown in Fig. 4e and Fig. 4f. It has been reported

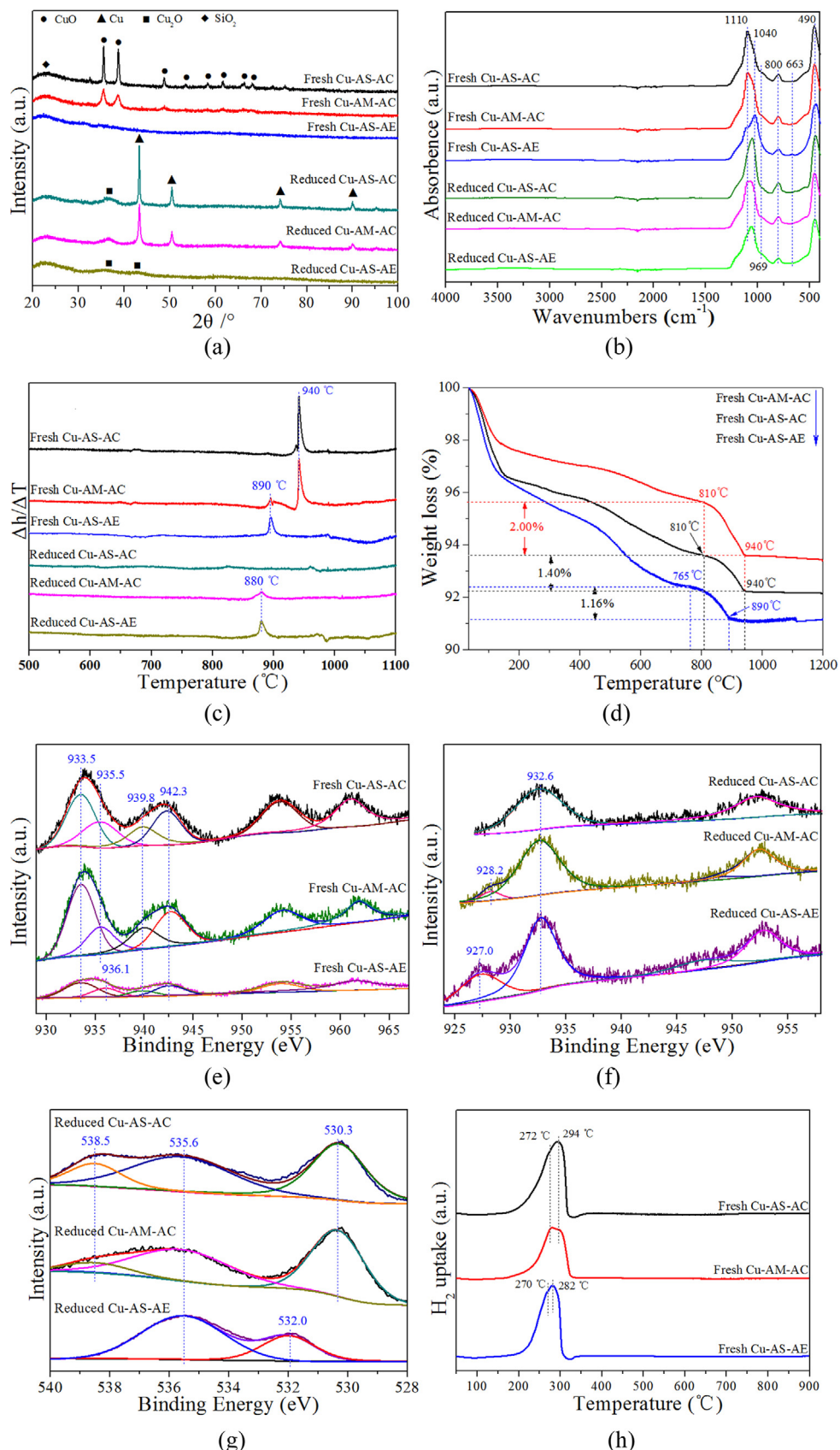
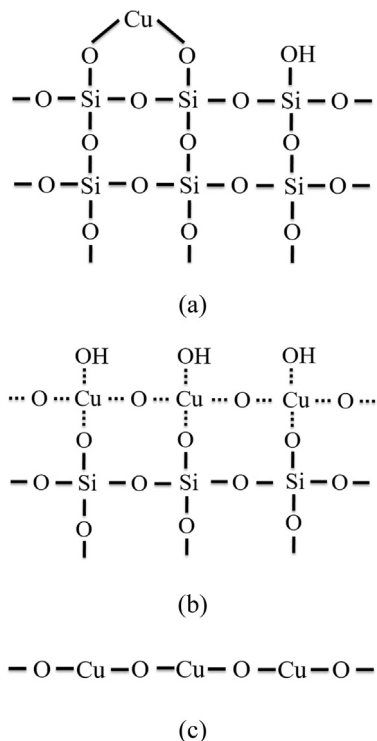


Fig. 4. Analysis of copper species in Cu-AS-AC, Cu-AM-AC and Cu-AS-AE. (a) XRD patterns; (b) IR spectra; (c) $\Delta h/\Delta T$ function as the temperature; (d) Weight loss function as the temperature; (e) Cu2p XPS spectra of fresh catalysts; (f) Cu2p XPS spectra of reduced catalysts; (g) O1s XPS of reduced catalysts; (h) H₂-TPR profiles of fresh and reduced catalysts.



Scheme 2. Molecular structures of (a) Cu—O—Si units, (b) copper phyllosilicate and (c) CuO.

that the peaks at 933.6 eV and 953.7 eV are attributed to Cu2p3/2 and Cu2p1/2 of Cu²⁺, respectively. Generally, the satellite peak between 939.5 eV and 943.5 eV can be assigned to Cu²⁺ as well [1,53]. The peaks at 932.7 eV and 952.5 eV are attributed to Cu2p3/2 and Cu2p1/2 of Cu⁺, respectively [54,55]. The peak corresponding to copper phyllosilicate is generally observed at 936.1 eV [28]. The peaks at 933.5 eV, 939.8 eV and 942.3 eV corresponding to Cu²⁺ are observed in the fresh catalysts. Notably, an apparent peak at 936.1 eV is observed in Cu-AS-AE, suggesting the existence of copper phyllosilicate, which is in agreement with the results of XRD, TEM and IR spectra. However, a peak at 935.5 eV is observed in Cu-AS-AC and Cu-AM-AC, which is most probably assigned to the ion-exchanged Cu—O—Si units, as the IR spectra suggested. The structures of ion-exchanged Cu—O—Si units, copper phyllosilicate and CuO have been shown in Scheme 2a–c. The model has been reported in previous literatures [44,53,56], and the structure of copper phyllosilicate is further explained in the supporting information (S3). The electron density of Cu in ion-exchanged Cu—O—Si units was between copper phyllosilicate and CuO, because the electron density around O decreased as follows: —OCu > —OSi > —OH [53]. Higher electron density indicates lower binding energies [57,58]. This further confirms the binding energy of ion-exchanged Cu—O—Si units at 535.5 eV. After reduction, Cu-AS-AC only shows the peak at 932.6 eV and 952.7 eV corresponding to Cu⁰ and Cu⁺, indicating that the copper species including CuO and ion-exchanged Cu—O—Si units were completely reduced. The reduced Cu-AS-AE not only shows the peaks corresponding to Cu⁰ and Cu⁺ but also exhibits the peak at 927.0 eV. Several previous papers have also reported the peak at ~927.0 eV, and all of them attributed this peak to the copper complex with high electron density [59–61]. In the present study, we attributed this peak to the reduced copper phyllosilicate, whose Cu²⁺—O—Si units were reduced to Cu⁺—O—Si units as indicated in previous papers [21,36]. From the IR spectra, the peak at 969 cm⁻¹ corresponding

to Cu—O—Si structures are apparently observed in the reduced Cu-AS-AE, possibly confirming the presence of Cu⁺—O—Si units in the reduced copper phyllosilicate. This is in agreement with previous work, which reported that copper phyllosilicate is easily reduced to Cu⁺ [21,28]. The peak at 938.2 eV in Cu-AM-AC is also attributed to the Cu⁺—O—Si units in the reduced copper phyllosilicate. The deviation of binding energies between Cu-AS-AE and Cu-AM-AC is most probably attributed to the difference in the extent of aggregation of copper phyllosilicate. The Cu⁺ species have several forms such as Cu₂O and Cu⁺—O—Si units. To ascertain which is the main form, the O1s XPS of reduced catalysts was conducted, as shown in Fig. 4g. The peak at 530.3 eV was observed in the reduced Cu-AS-AC and Cu-AM-AC, ascribed to Cu₂O as reported [62,63]. These observations indicate that the main form of Cu⁺ was Cu₂O for the reduced Cu-AS-AC and Cu-AM-AC. However, the Cu₂O peak was not observed, but a new peak at 532.0 eV appeared in reduced Cu-AS-AE, further suggesting the generation of Cu⁺—O—Si units because the electron density of O in Cu⁺—O—Si was lower than that in Cu₂O. The peaks at 535.6 eV and 538.5 eV are attributed to the O in SiO₂ and chemically adsorbed O, respectively [64]. It should be noted that the Cu—O—Si units in Cu-AS-AC were reduced to Cu₂O, whereas the copper phyllosilicate was reduced into Cu⁺—O—Si units. Being different from the Cu—O—Si units in Cu-AS-AC, a strong interaction existed between Cu and Cu in copper phyllosilicate (Scheme 2b and Fig. S2), so the structures and properties of Cu⁺—O—Si units reduced from copper phyllosilicate are different from the Cu—O—Si units even though both show the IR peak at 969 cm⁻¹. For example, the Cu—O—Si units do not show any peaks in TGA analysis, but the Cu⁺—O—Si units reduced from copper phyllosilicate do.

3.3.5. H₂-TPR analysis

Different copper species may have different electron density around copper, thus resulting in different reduction temperatures by H₂. Therefore, the H₂-TPR profiles of the fresh Cu-AS-AC, Cu-AM-AC and Cu-AS-AE were conducted and displayed in Fig. 4h. Cu-AS-AC and Cu-AM-AC present two reduction peaks at 272 °C and 294 °C, which correspond to the well dispersed CuO including ion-exchanged Cu—O—Si units and bulk CuO, respectively, agreeing with the previous studies [1,17,35]. Cu-AS-AE exhibits two peaks at 270 °C and 282 °C corresponding to the well dispersed CuO from the decomposition of copper phyllosilicate and the copper phyllosilicate, respectively. It is obvious that the Cu/SiO₂ prepared by (NH₄)₂CO₃ DPM increases the reduction temperature compared with the ones prepared by AEM. The different reduction temperatures for CuO may be attributed to the different sizes and shapes of the particles produced by different preparation methods. The results of the present study showed that copper phyllosilicate is partially reduced to Cu₂O, as the XRD patterns suggested, and some of them are reduced to Cu⁺—O—Si units, as the IR spectra, O1s XPS and TGA analysis indicated; on the other hand, ion-exchanged Cu—O—Si units are completely reduced to Cu₂O. The values of reduction peaks of well dispersed CuO and copper phyllosilicate are controversial. Some have reported the same reduction temperature for copper phyllosilicate and well dispersed CuO [1,21]. Others have reported lower reduction temperature for well dispersed CuO compared with copper phyllosilicate [65,66]. In the present study, we are inclined to agree with the latter results because the electron density of O in the CuO is higher than that of copper phyllosilicate (as shown in Scheme 2a–c), which might be more readily combined with H₂.

Most importantly, fresh Cu-AS-AE tended to generate large amount of copper phyllosilicate with a small amount of well dispersed CuO. The fresh Cu-AS-AC contained well dispersed CuO, ion-exchanged Cu—O—Si units and bulk CuO. The fresh Cu-AM-AC had bulk CuO, well dispersed CuO and ion-exchanged Cu—O—Si units with a small amount of copper phyllosilicate. The reduced Cu-

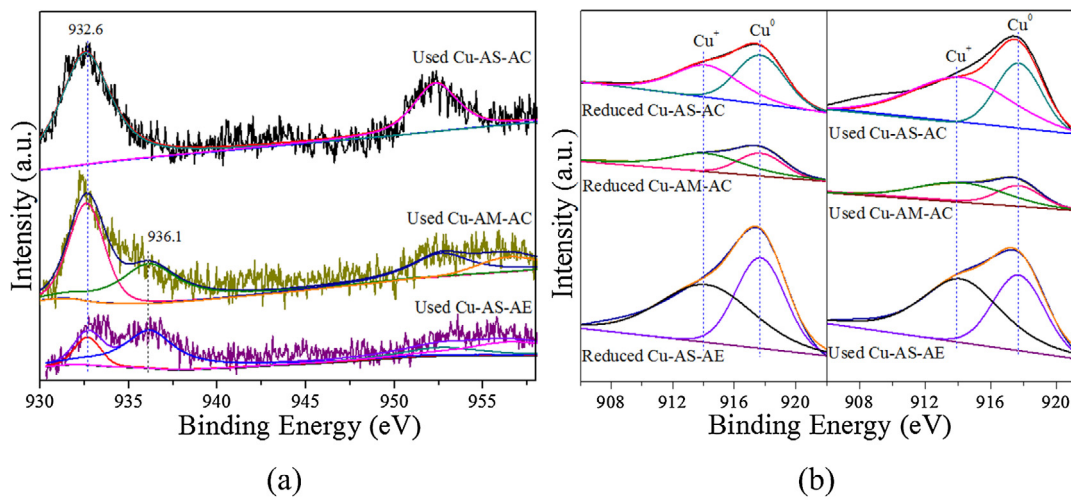


Fig. 5. Surface chemical states of catalysts (a) Cu2p XPS spectra of used catalysts; (b) XAES spectra of reduced and used catalysts.

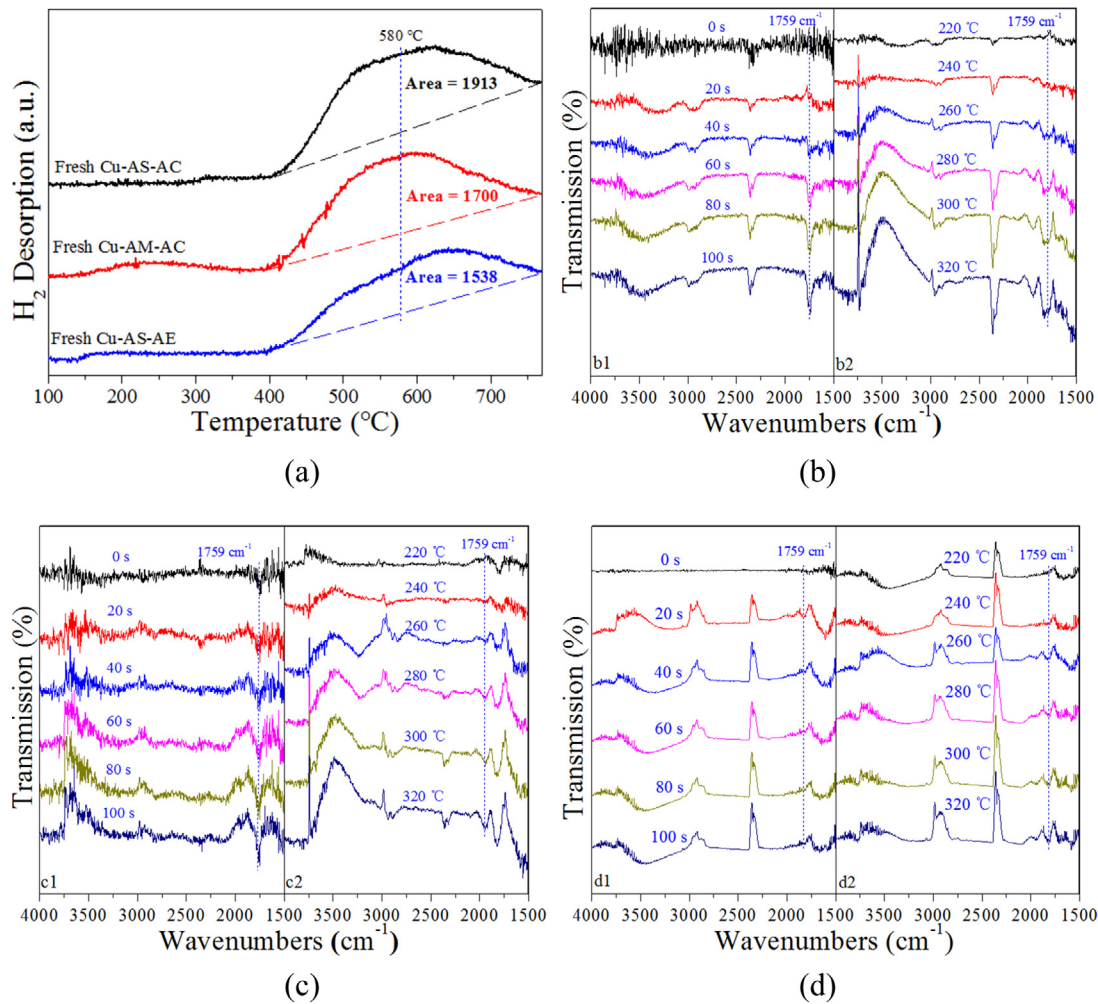


Fig. 6. Adsorption of H₂ and DEO on the catalysts. (a) H₂-TPD profiles of fresh Cu-AS-AC, Cu-AM-AC and Cu-AS-AE; (b) in situ FTIR of Cu-AS-AC; (c) in situ FTIR of Cu-AM-AC; (d) in situ FTIR of Cu-AS-AE.

AS-AC showed amounts of Cu⁰ and Cu₂O. The reduced Cu-AS-AE exhibited Cu⁰, Cu₂O and amounts of reduced copper phyllosilicate containing Cu⁺—O—Si units. The reduced Cu-AM-AC contained Cu⁰, Cu₂O with a small amount of reduced copper phyllosilicate.

3.4. Promotional mechanisms

From the above analysis, we can conclude that all the three catalysts had different copper species, possibly affecting the valence

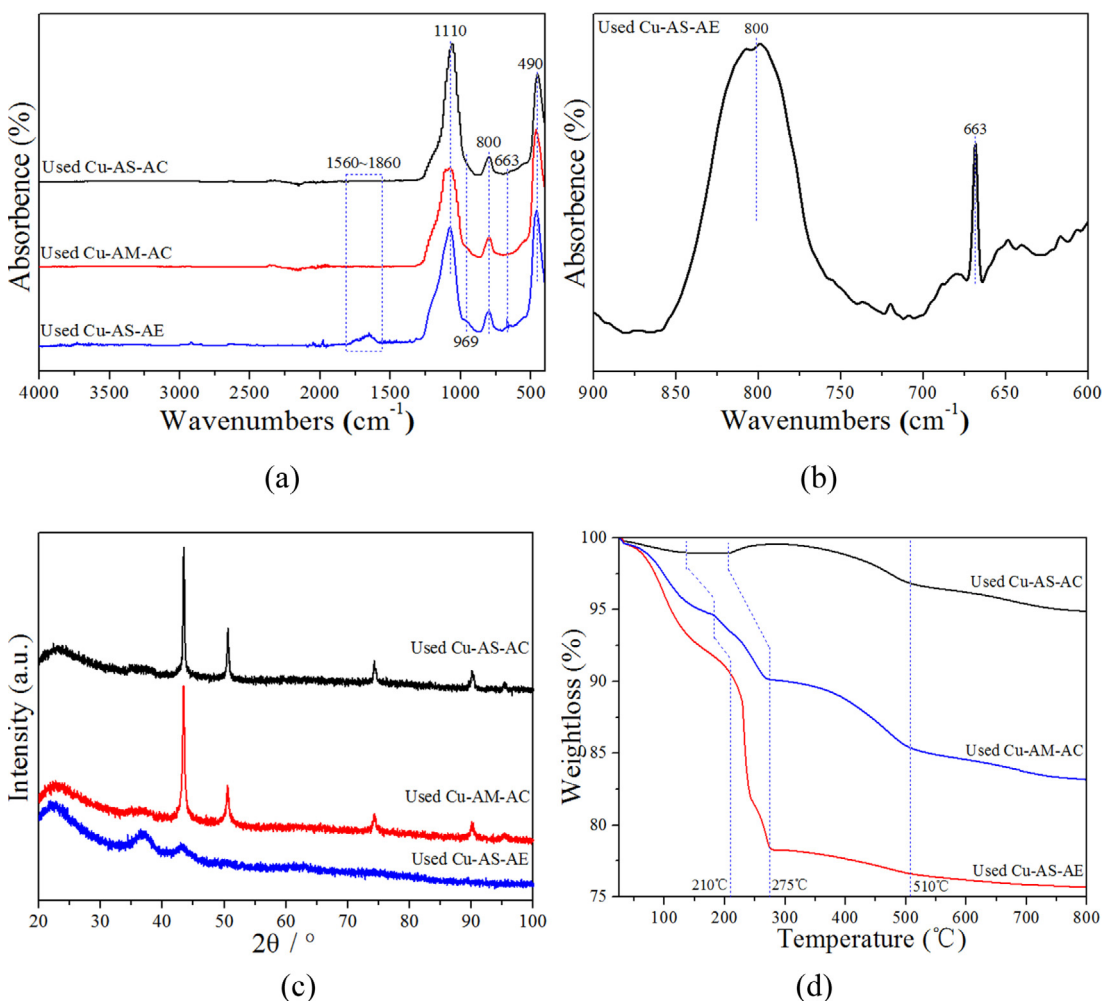


Fig. 7. Carbon deposition and stability of the catalysts (a) IR spectra of used catalysts; (b) the FTIR spectra ranging from 900 to 600 cm^{-1} of used Cu-AS-AE (c) XRD patterns of used catalysts; (d) TGA analysis of used catalysts under 80% N_2/O_2 .

states of copper species, which was reported to be a critical factor for the catalytic activities.

3.4.1. Surface chemical states of catalysts

The surface chemical states of catalysts play an important role in the hydrogenation reactions, which is affected by copper species present in the catalysts [19,21]. Therefore, the Cu2p XPS, O1s XPS and X-ray induced Auger spectra (XAES) of the reduced and used catalysts are shown in Figs. 4e–h and 5. In the Cu2p XPS, the used Cu-AS-AC only shows the peaks corresponding to Cu^+ , which exhibits almost no changes compared with the reduced one, indicating that the catalyst was stable in the vapor-phase DEO hydrogenation. However, being different from the reduced Cu-AS-AC and Cu-AS-AE, the peak at 936.1 eV corresponding to copper phyllosilicate can be observed for the used catalysts, and further the used Cu-AS-AE shows larger peaks of copper phyllosilicate. This may be caused by the oxidation of the $\text{Cu}^+ - \text{O} - \text{Si}$ units in the reduced copper phyllosilicate during the vapor-phase DEO hydrogenation, indicating that the Cu^+ in the reduced copper phyllosilicate is not stable in the reaction. Rode et al. has also found the oxidation of Cu species in the levulinic acid hydrogenation to γ -valerolactone [67].

The kinetic energies (KE) of the Cu LMM Auger electrons were employed to distinguish between the Cu^0 and Cu^+ species as shown in Fig. 5b. In general, the KE is ca. 917.9 eV for Cu^0 and 913.7 eV for Cu^+ . The deconvolution results are listed in Table 4. As shown in

Table 4, all three fresh catalysts showed a high Cu^{2+} concentration without Cu^0 and Cu^+ . However, the Cu^{2+} was completely eliminated after reduction, while the contents of Cu^+ and Cu^0 apparently increased. As it is well known, the Cu^+ concentration and the ratio of $\text{Cu}^+ / (\text{Cu}^+ + \text{Cu}^0)$ play an important role in the oxalate hydrogenation. Higher content and ratio mean higher catalytic activity [19,21,28]. Table 4 shows that the reduced Cu-AS-AC had the highest Cu^+ concentration and $\text{Cu}^+ / (\text{Cu}^+ + \text{Cu}^0)$ ratio, while the reduced Cu-AS-AE achieved the lowest. The used Cu-AS-AC shows a negligible decrease in the Cu^+ concentration and $\text{Cu}^+ / (\text{Cu}^+ + \text{Cu}^0)$ ratio, while the used Cu-AS-AE shows the largest decrease, and the used Cu-AM-AC exhibits a decrease in between, which is consistent with the results of the catalytic activities and long-term stability. This indicates the important role played by the Cu^+ concentration and $\text{Cu}^+ / (\text{Cu}^+ + \text{Cu}^0)$ ratio in the catalytic activities and long-term stability. The decreased values for the used catalysts, however, may be caused by the unstable $\text{Cu}^+ - \text{O} - \text{Si}$ units in reduced copper phyllosilicate.

3.4.2. Adsorption of H_2 and DEO

It is possible that the high Cu^+ concentration and $\text{Cu}^+ / (\text{Cu}^0 + \text{Cu}^+)$ ratio increase the catalytic performance via the adsorption of H_2 and DEO. H_2 surface adsorption behaviors on Cu-AS-AC, Cu-AM-AC and Cu-AS-AE were analyzed using the H_2 -TPD technique. The H_2 -TPD profiles of Cu-AS-AC, Cu-AM-AC and Cu-AS-AE, activated by H_2 at 623 K for 4 h, showed two desorption peaks at 150–300 °C

and 400–760 °C, respectively (Fig. 6a). As previously reported, H₂ desorption peaks in the low temperature ranges corresponded to chemisorbed H₂ on the metallic Cu surface [3], while the shoulder peak at 400–760 °C would arise from the split H–H on the surface of the catalysts [35,68]. From Fig. 6a, it can be deduced that the adsorption of split H–H on the surface of Cu-AS-AC is largest among the three catalysts, while that on Cu-AS-AE is the smallest, which is consistent with the catalytic activities, suggesting the important role of the split H–H adsorptions.

The *in situ* FTIR spectroscopy was employed as shown in Fig. 6b–d to study the DEO adsorption on the surfaces of Cu-AS-AC, Cu-AM-AC and Cu-AS-AE. In general, the bands at about 1759 cm⁻¹ and 1742 cm⁻¹ were assigned to the C=O stretching vibrations in the DEO. Fig. 6b1 shows that the peak intensity of DEO increased with the time, indicating that the DEO can be chemically and physically adsorbed on the surface of Cu-AS-AC. Fig. 6b2 illustrates that such adsorption increases further with the temperature, suggesting the main chemical adsorption of DEO on the surface of Cu-AS-AC. As the physical adsorption is weak, it should be desorbed with the temperature rising. Cu-AM-AC shows a similar change of peak intensity but it seems much weaker (Fig. 6c and Fig. S3), and Cu-AS-AE shows the weakest peaks among the three catalysts, indicating that the adsorption of DEO on Cu-AS-AE was the lowest (Fig. 6d). The differences probably resulted from the different content of Cu⁺ and from the Cu⁺/(Cu⁰+Cu⁺) ratio. Ma's group have reported that the Cu⁺ sites mainly adsorbed the organic compounds [29].

3.4.3. Carbon deposition

Good adsorption of DEO and H₂ may also result in carbon adsorption, which may affect the catalytic activities and long-term stability. Therefore, it was investigated systematically. The IR spectra of used Cu-AS-AC, Cu-AM-AC and Cu-AS-AE are shown in Fig. 7. All three used catalysts show apparent peaks at 1110 cm⁻¹, 800 cm⁻¹ and 490 cm⁻¹ corresponding to Si–O and Cu–O vibrations. The used Cu-AS-AE exhibits some additional peaks at 663 cm⁻¹, 969 cm⁻¹ and 1550–1830 cm⁻¹, which can be attributed to copper phyllosilicate, Cu⁺–O–Si units in reduced copper phyllosilicate and carbon depositions, respectively. Carbon deposition has also been observed by Sarbak et al. at ca. 1500–2000 cm⁻¹ [69,70]. However, the peaks at 663 cm⁻¹, 969 cm⁻¹ and 1550–1830 cm⁻¹ are hardly observed in Cu-AS-AC, indicating the stability of the catalyst. The appearance of the peak at 663 cm⁻¹ further indicates the unstable Cu⁺–O–Si units in reduced copper phyllosilicate of Cu-AS-AE during the vapor-phase DEO hydrogenation. Although the oxidation process occurred in hydrogenation, no CuO was generated, which can be observed from the XRD patterns of the used catalysts as shown in Fig. 7c, illustrating the stable Cu₂O in the hydrogenation.

The amount of carbon depositions for three catalysts was measured by TG analysis in the atmosphere of 80 v/v% N₂/20 v/v% O₂, as shown in Fig. 7d. There are four steps of weight loss in the whole temperature range. The first step at low temperature corresponds to the loss of surface H₂O. The second step at medium temperature is most probably attributed to the loss of carbon deposits. Many previous literatures have reported that the carbon deposit is oxidized in the temperature range of 200–400 °C [71–73]. It is interesting that the weight of used Cu-AM-AC and used Cu-AS-AE decreases very slowly even though the weight of used Cu-AS-AC increases in the third step. This decrease may be caused by the competition between Cu⁺ oxidation and the decomposition of the carbon deposition. The weight loss in the fourth step may be due to the decomposition of CuO. The present results indicate that the used Cu-AS-AE showed the most serious carbon deposition, and the used Cu-AS-AC showed almost no carbon deposition. As such,

copper phyllosilicate may benefit the deposition of carbon on the surface of catalysts possibly due to the large surface areas.

4. Conclusions

Cu/SiO₂ catalysts prepared by cost-effective and environmentally benign (NH₄)₂CO₃ DPM (Cu-AS-AC and Cu-AM-AC) were systematically characterized and compared with the catalysts prepared by AEM (Cu-AS-AE). Interestingly, Cu-AS-AC and Cu-AM-AC with lower BET surface area, poorer dispersion of copper species, and lower concentration of copper phyllosilicate and surface composition produced higher catalytic activities for vapor-phase DEO hydrogenation than Cu-AS-AE. Analysis of the copper species indicated that Cu-AS-AC contains ion-exchanged Cu–O–Si units that are beneficial for generating stable Cu₂O, resulting in high Cu⁺ concentration, Cu⁺/(Cu⁰+Cu⁺) ratio, and adsorption of DEO and H₂. These attribute collectively promote the catalytic activity and stability. Further, compared to Cu₂O in Cu-AS-AC, the Cu⁺–O–Si units from the reduced Cu-AS-AE are unstable and easily oxidized to copper phyllosilicate during the vapor-phase DEO hydrogenation. Apparently, the copper phyllosilicate from Cu-AS-AE enhances the formation of carbon deposition. Both instability and carbon deposition result in the deactivation during the vapor-phase DEO hydrogenation.

Acknowledgements

This work is financially supported by the U.S. Department of Energy, State of Wyoming and China Scholarship Council.

Appendix A. Supplementary data

Supplementary data associated with this article can be found, in the online version, at <http://dx.doi.org/10.1016/j.apcatb.2017.02.072>.

References

- [1] J. Zheng, J. Zhou, H. Lin, X. Duan, C.T. Williams, Y. Yuan, *J. Phys. Chem. C* 119 (2015) 13758–13766.
- [2] Y. Huang, H. Ariga, X. Zheng, X. Duan, S. Takakusagi, K. Asakura, Y. Yuan, *J. Catal.* 307 (2013) 74–83.
- [3] J. Ding, J. Zhang, C. Zhang, K. Liu, H. Xiao, F. Kong, J. Chen, *Appl. Catal. A* 508 (2015) 68–79.
- [4] L. Han, G. Zhao, Y. Chen, J. Zhu, P. Chen, Y. Liu, Y. Lu, *Catal. Sci. Technol.* (2016), <http://dx.doi.org/10.1039/c6cy01361>.
- [5] J. Zhou, X. Duan, L. Ye, J. Zheng, M.M.J. Li, S.C.E. Tsang, Y. Yuan, *Appl. Catal. A* 505 (2015) 344–353.
- [6] Y. Liu, J. Ding, J. Sun, J. Zhang, J. Bi, K. Liu, F. Kong, H. Xiao, Y. Sun, J. Chen, *Chem. Commun.* 52 (2016) 5030–5032.
- [7] C. Wen, Y. Cui, X. Chen, B. Zong, W. Dai, *Appl. Catal. B* 162 (2015) 483–493.
- [8] X. Kong, C. Ma, J. Zhang, J. Sun, J. Chen, K. Liu, *Appl. Catal. A* 509 (2016) 153–160.
- [9] L. Han, L. Zhang, G. Zhao, Y. Chen, Q. Zhang, R. Chai, Y. Liu, Y. Lu, *ChemCatChem* 8 (2016) 1065–1073.
- [10] Y. Cui, B. Wang, C. Wen, X. Chen, W. Dai, *ChemCatChem* 8 (2016) 527–531.
- [11] H. Adkins, E.E. Burgoyne, H.J. Schneider, *J. Am. Chem. Soc.* 72 (1950) 2626–2629.
- [12] H. Yue, Y. Zhao, L. Zhao, J. Lv, S. Wang, J. Gong, X. Ma, *AIChE J.* 58 (2012) 2798–2809.
- [13] B. Wang, Y. Cui, C. Wen, X. Chen, Y. Dong, W.L. Dai, *Appl. Catal. A* 509 (2016) 66–74.
- [14] J. Ding, Y. Liu, J. Zhang, K. Liu, H. Xiao, F. Kong, Y. Sun, J. Chen, *Catal. Sci. Technol.* (2016), <http://dx.doi.org/10.1039/c6cy0071se>.
- [15] B. Wang, C. Wen, Y. Cui, X. Chen, Y. Dong, W. Dai, *RSC Adv.* 5 (2015) 29040–29047.
- [16] J. Ding, J. Chen, *RSC Adv.* 5 (2015) 82822–82833.
- [17] S. Zhao, H. Yue, Y. Zhao, B. Wang, Y. Geng, J. Lv, S. Wang, J. Gong, X. Ma, *J. Catal.* 297 (2013) 142–150.
- [18] C. Wen, Y. Cui, W. Dai, S. Xie, K. Fan, *Chem. Commun.* 49 (2013) 5195–5197.
- [19] A. Yin, X. Guo, W. Dai, K. Fan, *J. Phys. Chem. C* 113 (2009) 11003–11013.
- [20] H. Lin, X. Zheng, Z. He, J. Zheng, X. Duan, Y. Yuan, *Appl. Catal. A* 445–446 (2012) 287–296.

- [21] L. Chen, P. Guo, M. Qiao, S. Yan, H. Li, W. Shen, H. Xu, K. Fan, *J. Catal.* 257 (2008) 172–180.
- [22] A. Yin, X. Guo, K. Fan, W.L. Dai, *Appl. Catal. A* 377 (2010) 128–133.
- [23] W. Di, J. Cheng, S. Tian, J. Li, J. Chen, Q. Sun, *Appl. Catal. A* 510 (2016) 244–259.
- [24] J. Lin, X. Zhao, Y. Cui, H. Zhang, D. Liao, *Chem. Commun.* 48 (2012) 1177–1179.
- [25] Y. Zhu, Y. Zhu, G. Ding, S. Zhu, H. Zheng, Y. Li, *Appl. Catal. A* 468 (2013) 296–304.
- [26] L. Zhang, Y. Zhang, S. Chen, *Appl. Catal. A* 415–416 (2012) 118–123.
- [27] C. Wen, A. Yin, Y. Cui, X. Yang, W. Dai, K. Fan, *Appl. Catal. A* 458 (2013) 82–89.
- [28] J. Gong, H. Yue, Y. Zhao, S. Zhao, L. Zhao, J. Lv, S. Wang, X. Ma, *J. Am. Chem. Soc.* 134 (2012) 13922–13925.
- [29] Y. Wang, Y. Shen, Y. Zhao, J. Lv, S. Wang, X. Ma, *ACS Catal.* 5 (2015) 6200–6208.
- [30] T. Popa, Y. Zhang, E. Jin, M. Fan, *Appl. Catal. A* 505 (2015) 52–61.
- [31] B. Wang, X. Zhang, Q. Xu, G. Xu, *Chin. J. Catal.* 29 (2008) 275–280.
- [32] C. Ziebart, R. Jackstell, M. Beller, *ChemCatChem* 5 (2013) 3228–3231.
- [33] A. Yin, C. Wen, X. Guo, W. Dai, K. Fan, *J. Catal.* 280 (2011) 77–88.
- [34] S. Zhu, X. Gao, Y.L. Zhu, Y.F. Zhu, H. Zheng, Y. Li, *J. Catal.* 303 (2013) 70–79.
- [35] X. Zheng, H. Lin, J. Zheng, X. Duan, Y. Yuan, *ACS Catal.* 3 (2013) 2738–2749.
- [36] X. Ma, H. Chi, H. Yue, Y. Zhao, Y. Xu, J. Lv, S. Wang, J. Gong, *AIChE J.* 59 (2013) 2530–2539.
- [37] R. Rameshan, L. Mayr, B. Klotzer, D. Eder, A. Knop-Gericke, *J. Phys. Chem. C* 119 (2015) 26948–26958.
- [38] Q. Yao, Z. Lu, Z. Zhang, X. Chen, Y. Lan, *Sci. Rep.* 4 (2014) 1–8.
- [39] H. Yue, Y. Zhao, S. Zhao, B. Wang, X. Ma, J. Gong, *Nat. Commun.* 4 (2013) 1–7.
- [40] Z. Huang, F. Cui, J. Xue, J. Zuo, J. Chen, C. Xia, *J. Phys. Chem. C* 114 (2010) 16104–16113.
- [41] X. Dong, X. Ma, H. Xu, Q. Ge, *Catal. Sci. Technol.* 6 (2016) 4151–4158.
- [42] A. Yin, X. Guo, K. Fan, W. Dai, *Appl. Catal. A* 377 (2010) 128–133.
- [43] S. Wang, X. Li, Q. Yin, L. Zhu, Z. Luo, *Catal. Commun.* 12 (2011) 1246–1250.
- [44] T. Toupane, M. Kermarec, J.F. Lamber, C. Louis, *J. Phys. Chem. B* 106 (2002) 2277–2286.
- [45] L. Lu, X. Huang, *Microchim. Acta* 175 (2011) 151–157.
- [46] J. Maul, A.S. Brito, A.L. de Oliveira, S.J.G. Lima, M.A.A. Maurera, D. Keyson, A.G. Souza, I.M.G. Santos, *J. Therm. Anal. Calorim.* 106 (2011) 519–523.
- [47] Y. Kong, H. Zhu, G. Yang, X. Guo, W. Hou, Q. Yan, M. Gu, C. Hu, *Adv. Funct. Mater.* 14 (2014) 816–820.
- [48] C. Huo, J. Ouyang, H. Yang, *Sci. Rep.* 4 (2014) 1–9.
- [49] H. Kobayashi, N. Takezawa, C. Minochi, K. Takahashi, *Chem. Lett.* (1980) 1197–1200.
- [50] M.A. Kohler, J.C. Lee, D.L. Trimm, N.W. Cant, M.S. Wainwright, *Appl. Catal. B* 31 (1987) 309–312.
- [51] D. Chadda, J.D. Ford, *Int. J. Energy Res.* 13 (1989) 63–73.
- [52] R.L. Frost, Y. Xi, *J. Therm. Anal. Calorim.* 112 (2013) 615–619.
- [53] Y.H. Kim, D.K. Lee, H.G. Cha, C.K. Kim, Y.C. Kang, Y.S. Kang, *J. Phys. Chem. B* 110 (2006) 24923–24928.
- [54] J.P. Espinos, J. Morales, A. Barranco, A. Caballero, J.P. Holgado, A.R. Gonzalez-Elipe, *J. Phys. Chem. B* (2002) 6921–6929.
- [55] G. Panzner, B. Egert, H.P. Schmidt, *Surf. Sci.* 151 (1985) 400–408.
- [56] M.G. da Fonseca, C. Airolidi, *J. Mater. Chem.* 10 (2000) 1457–1463.
- [57] J. Ding, Q. Zhong, S. Zhang, *Ind. Eng. Chem. Res.* 54 (2015) 2012–2022.
- [58] J. Ding, Q. Zhong, H. Cai, S. Zhang, *Chem. Eng. J.* 286 (2016) 549–559.
- [59] H. Liu, Z. Huang, Z. Han, K. Ding, H. Liu, C. Xia, J. Chen, *Green Chem.* 17 (2015) 4281–4290.
- [60] W. Yang, J.J. Gooding, D.B. Hibbert, *J. Electroanal. Chem.* 516 (2001) 10–16.
- [61] F. Rochet, G. Dufour, H. Roulet, N. Motta, A. Sgarlata, M.N. Piancastelli, M.D. Crescenzi, *Surf. Sci.* 319 (1994) 10–20.
- [62] K. Tang, X. Wang, W. Yan, J. Yu, R. Xu, *J. Membr. Sci.* 286 (2006) 279–284.
- [63] P. Jiang, D. Prendergast, F. Borondics, S. Porgaard, L. Giovanetti, E. Pach, J. Newberg, H. Bluhm, F. Besenbacher, M. Salmeron, *J. Chem. Phys.* 138 (2013) 024704-1–024704-6.
- [64] Y.H. Kim, D.K. Lee, H.G. Cha, C.W. Kim, Y.S. Kang, *J. Phys. Chem. C* 111 (2007) 3625–3629.
- [65] C.J.G. Van Der Grift, A.F.H. Wielers, A. Mulder, J.W. Geus, *Thermochim. Acta* 171 (1990) 95–113.
- [66] J.Y. Carriat, M. Che, M. Kermarec, *Catal. Lett.* 25 (1994) 127–140.
- [67] A.M. Hengne, C.V. Rode, *Green Chem.* 14 (2012) 1064–1072.
- [68] A.G. Boudjahem, S. Monteverdi, M. Mercy, D. Ghanbaja, M.M. Bettahar, *Catal. Lett.* 84 (2002) 115–122.
- [69] Z. Sarbak, *Appl. Catal. A* 177 (1999) 85–97.
- [70] K. Tomishige, Y. Chen, K. Fujimoto, *J. Catal.* 181 (1999) 91–103.
- [71] V. Alzate-Restrepo, J.M. Hill, *Appl. Catal. A* 342 (2008) 49–55.
- [72] J. Ali, S.D. Jackson, *Appl. Petrochem. Res.* 4 (2014) 33–39.
- [73] D.J. Moodley, J. van de Loosdrecht, A.M. Said, M.J. Overett, A.K. Datye, J.W. Niemantsverdriet, *Appl. Catal. A* 354 (2009) 102–110.